Photonic Band Gap Materials: A Semiconductor for Light

Sajeev John[1], Ovidiu Toader[1], and Kurt Busch[2]

Abstract

Light in certain engineered dielectric microstructures can flow in a way similar to electrical currents in semiconductor chips. These microstructures represent a new frontier in the field of optics. They provide a foundation for the development of novel micro-photonic devices and the integration of such devices into an optical microchip.

1 Introduction

Electromagnetism is the fundamental mediator of all interactions in atomic physics and condensed matter physics, in other words, the force that governs the structure of ordinary matter. In a novel class of engineered dielectric materials known as photonic band gap (PBG) materials, a fundamentally new electromagnetic effect can be realized. This phenomenon is the localization of light [1,2] and it may prove central to the utilization of light waves for information and communication technologies.

In the nineteenth century, James Clerk Maxwell deduced a precise and elegant mathematical description of the propagation of light. Maxwell's theory of electromagnetic wave propagation was shortly thereafter tested and verified by Heinrich Hertz. There began the age of wireless communication. This allowed ships at sea to communicate with land. Today, the same basic discovery provides us with the use of radio, television, and mobile phones. Despite the widespread knowledge and use of Maxwell's theory of electromagnetism, it has only recently been recognized that light waves not only propagate, they can also be trapped.

The invention of the laser in the latter half of the 20th century was another milestone in the science and technology of light. Laser light allows us to probe the structure of matter with unprecedented accuracy, it provides medical practitioners with a cutting tool sharper than any surgeon's knife and allows us to modulate communication signals for high speed data transfer along the internet. Today, using laser light, undersea fiber optic cables carry enormous amounts of voice communications and data with such clarity that a pin drop in Karlsruhe, Germany can be heard clearly in Toronto, Canada.

Optical fibers are replacing electrical wires in shorter distance communications such as local access networks and computer to computer communications. In a completely seamless network, communications between nearby computer chips and even within a single computer chip would take place with tiny beams of laser light rather than electricity. Optical computers of this type may be faster and support neural architectures (circuit interconnections resembling that of a human brain) unlike their electronic counterparts which are restricted in architecture due to electrical cross-talk between nearby wires. That is to say, electrical current in one wire can disturb electrical signals

---

[1] Department of Physics, University of Toronto, 60 St. George Street, Toronto, Ontario, M5S-1A7,Canada
[2] Institut für Theorie der Kondensierten Materie, Universität Karlsruhe, 76128 Karlsruhe, Germany

passing through nearby wires. Laser beams, on the other hand, can co-exist without disrupting one another.

The trapping and micro-moulding of light flow needed for the applications suggested above requires materials which can scatter light much more strongly than any naturally occurring material. We experience multiple light scattering when it becomes dark on a cloudy day. Light from the sun scatters many times from water droplets, following a tortuous diffusion path before reaching the ground. The distance the light travels within the cloud before it is scattered into a random direction is called the mean free path. The effect of multiple scattering is that the amount of light transmitted through the cloud is reduced by a factor of the ratio of the cloud thickness to the mean free path. The rest comes back out the other side, which is why clouds appear white. Multiple light scattering also takes place in human tissue. Here the transport mean free path for light of one micrometer wavelength is about a millimeter.

But neither clouds nor human tissue can scatter light sufficiently strongly to localize light. For this to happen a collection of microscopic dielectric structures that scatter light a thousand times more strongly than human tissue is required. In this case the transport mean free path becomes as short as the wavelength of light itself. If, in addition to the strong resonant scattering of the individual dielectric particles, there is a periodic arrangement of the scatterers, then pathways for light propagation over specific frequency intervals can be completely removed. The removal of pathways over all directions over a band of frequencies is referred to as the creation of a photonic band gap (PBG). Dielectric microstructures that exhibit this effect are called PBG materials.

In electronic micro-circuits, electrical currents are guided by thin metal wires. Electrons are bound within the cross section of the wire by the so-called work function (confining potential) of the metal. As a result, electrical currents follow the path prescribed by the wire without escaping into the background. The situation is very different for optical waves. Although optical fibers guide light over long distances, micro-circuits of light based on fibers do not exist. This is because empty space is already an ideal conductor of light waves. The light in an optical fiber can easily escape into the background electromagnetic modes of empty space if the fiber is bent or distorted on a microscopic scale. PBG materials remove this problem by removing all the background electromagnetic modes over the relevant band of frequencies. Light paths can be created inside a PBG material in the form of engineered waveguide channels. The PBG localizes the light and prevents it from escaping the optical micro-circuit.

The question of whether light can be localized can be posed in the form of an analogy between Maxwell's equations for electromagnetic wave propagation and Schrödinger's equation for electrons propagating in a scattering potential. Consider a monochromatic electromagnetic wave of frequency ω propagating in a medium whose dielectric constant varies from point to point in space as:

$$\varepsilon(x) = \varepsilon_0 + \varepsilon_{\text{fluct}}(x) \tag{1}$$

Here, ε_0 is the average part of the dielectric constant and $\varepsilon_{\text{fluct}}(x)$ represents the part of the dielectric constant that varies from point to point in space. We assume that the dielectric microstructure does not absorb the light and that the total dielectric constant is everywhere real and positive. The wave equation for such an optical field is given by:

$$-\nabla^2 \vec{E} + \vec{\nabla}(\vec{\nabla} \cdot \vec{E}) - \frac{\omega^2}{c^2}\varepsilon_{\text{fluct}}(x)\vec{E} = \frac{\omega^2}{c^2}\varepsilon_0 \vec{E} \qquad (2)$$

Equation (2) has been written in a form which resembles the quantum mechanical Schrödinger equation. Here, the first two terms are the analogues of the "kinetic energy" terms in Schrödinger's equation, $(\omega^2/c^2)\varepsilon_{fluct}(x)$ plays the role of a scattering potential, and $(\omega^2/c^2)\varepsilon_0$ is analogous to an energy eigenvalue. The Maxwell wave equation (2) describes a vector wave field as opposed to complex scalar wave-function in Schrödinger's equation.

The essential subtlety of light localization is apparent from equation (2). Unlike electrons which can be trapped and localized for negative eigenvalues (bound states) in corresponding negative energy potential wells, the overall positivity of the dielectric constant (1) leads to the constraint that the energy eigenvalue, $(\omega^2/c^2)\varepsilon_0$, is always greater than the highest of the potential barriers presented by $(\omega^2/c^2)\varepsilon_{fluct}(x)$. The occurrence of bound states of the electromagnetic wave field in this spectral range requires extremely specialized and artificially engineered dielectric materials.

2. Photonic Band Gap Formation

PBG materials were predicted theoretically as a means to realize the localization and trapping of light in a bulk material over a band of frequencies [3]. A direct corollary of this principle is the complete inhibition of spontaneous emission [4,5] from an atom, molecule, or electron-hole pair excitation that is placed within the PBG material. Indeed, if the emission frequency from the atom lies within the PBG, the photon that would normally be emitted forms a bound state to the atom. Nearly all of the novel consequences of PBG materials are a direct consequence of these remarkable effects. Unlike optical confinement of a single resonance mode in a high quality (Q factor) optical cavity, localized electromagnetic modes in a bulk PBG material are completely decoupled from the vacuum modes of free space. Unlike well known layered dielectric structures (including Fabry-Perot resonators and distributed feedback laser cavities) which may confine light in one spatial dimension, the PBG material facilitates coherent localization of light in all spatial directions. This unique combination of light localization and the complete control of radiative dynamics distinguishes PBG materials from any previously studied optical system.
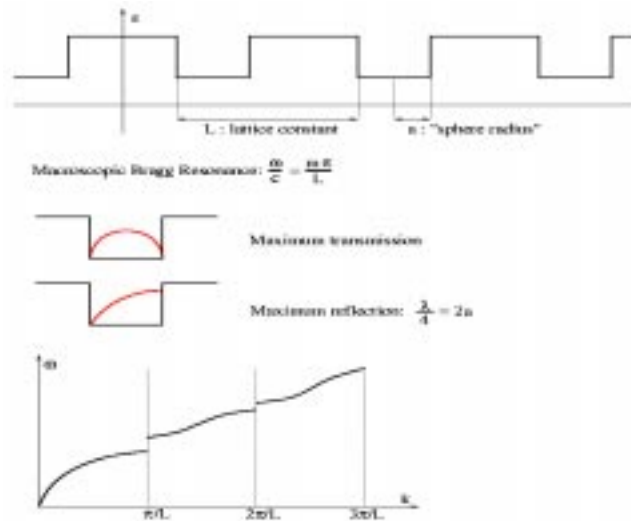
Figure 1. PBG formation can be regarded as the synergetic interplay between two distinct resonance scattering mechanisms. The first is the "macroscopic" Bragg resonance from a periodic array of scatterers. This leads to electromagnetic stop gaps when the wave propagates in the direction of periodic modulation when an integer number, m=1,2,3…, of half wavelengths coincides with the lattice spacing, L, of the dielectric microstructure. The second is a "microscopic" scattering resonance from a single unit cell of the material. In the illustration, this (maximum backscattering) occurs when precisely one quarter of the wavelength coincides with the diameter, 2a, of a single dielectric well of refractive index n. PBG formation is enhanced by choosing the materials parameters a, L, and n such that both the macroscopic and microscopic resonances occur at the same frequency.

Photonic band gap formation can be understood as a synergetic interplay between two distinct resonance scattering mechanisms. One is the microscopic scattering resonance from the dielectric material contained in a single unit cell of the photonic crystal. A simple illustration of this is provided (**Figure 1**) by the scattering of a wave from a square well potential. When one half of the optical wavelength fits into the width of the well, the transmission of light from left to right is maximum and the least light is reflected. When one quarter of a wavelength fits into the width of the well, the least amount of light is transmitted and the maximum amount of light is reflected. This quarter wavelength condition is a simple example of the condition for a microscopic scattering resonance. The second resonance is macroscopic resonance from the geometrical arrangement of the repeating unit cells of the dielectric microstructure. If there is a periodic arrangement of unit cells, this is called Bragg scattering. This occurs whenever the spacing between adjacent unit cells is an integer multiple of half of the optical wavelength. Photonic band gap formation is facilitated if the geometrical parameters of the photonic crystal are chosen so that both the microscopic and macroscopic resonances occur at precisely the same wavelength. In addition, both of these scattering mechanisms must individually be quite strong. In practice, this means that the underlying solid material must have a very high refractive index (typically about 3.0 or higher) while at the same time exhibit negligible absorption or extinction of the light (less than 1 decibel of attenuation over a centimeter). These conditions on the scattering strength, the geometry, and the purity the dielectric material severely restrict the set of engineered dielectrics that exhibit a PBG. Candidate materials for the PBG backbone include silicon, germanium, gallium arsenide, and indium phosphide.
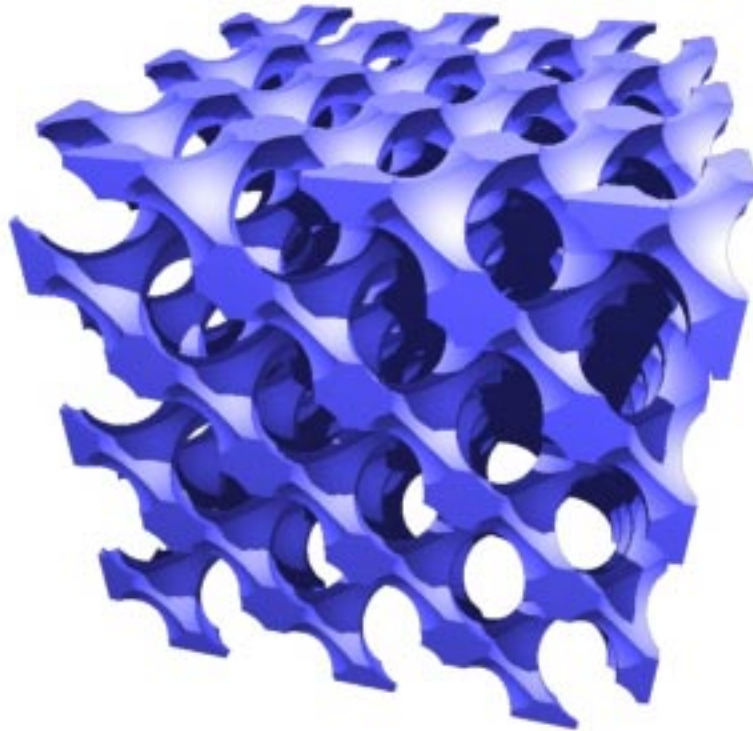
Figure 2. The "inverted diamond" structure was one of the first prototype structures predicted to exhibit a large and robust 3D PBG. It consists of an overlapping array of air spheres arranged in a diamond lattice. This structure can be mimicked by drilling an array of criss-crossing cylindrical holes into a bulk dielectric. The solid backbone consists of a high refractive index material such as silicon leading to a 3D PBG as large as 27% of the center frequency. The minimum refractive index (of the backbone) for the emergence of a PBG is roughly 2.0. Practical difficulties in the synthesis of this structure have motivated simpler but closely related designs such as the "woodpile " structure (see **Figure 9**).

Scalar waves (sound waves and other compression waves in solids) readily exhibit complete three-dimensional gaps for simple structures such as a face-centered cubic (FCC) lattice of spherical scatterers [6]. In contrast, electromagnetic waves involve three component electric and magnetic field vectors. This leads to much more restrictive conditions on the dielectric constant, the solid volume fraction, and the microstructure connectivity for the formation of a PBG. One very widely studied class of PBG materials is that based on a diamond lattice of dielectric scatterers. For example, a diamond lattice of very high dielectric constant, nonoverlapping spheres exhibits a PBG for which electromagnetic wave propagation is completely forbidden over a narrow frequency band [7]. An "inverse diamond" lattice of overlapping air spheres in a high refractive index background (**Figure 2**) exhibits a much larger PBG. In the microwave regime, other diamond-like structures obtained by drilling cylindrical holes in a bulk dielectric material (with refractive index of 3.5) have been demonstrated to exhibit band-gap to center frequency ratios as large as 20% [8]. Since then, numerous structures amenable to layer by layer fabrication have been suggested, the most notable being the "woodpile" structure [9,10,11,12]. A number of structures have already been fabricated with PBG's in the range of millimeter waves [13,14,15]. The diamond structure and its cousins constitute a

family of PBG materials which are characterized by a large and complete PBG between the second and third bands (fundamental gap) in the photonic band structure. The FCC lattice structure, on the other hand, does not exhibit a complete PBG between the 2nd and 3rd bands. Instead it has a small PBG between the 8th and 9th bands. While it has been a common belief that only the diamond structure is associated with large and complete PBG's, very recently a new class of microstructures based on a tetragonal lattice has been discovered that exhibits a large PBG between the 4th and 5th electromagnetic dispersion bands [O. Toader and S. John to be published]. An illustration of such a lattice consisting of square spiral posts is shown in **Figure 3**. When the posts are made of silicon, this structure exhibits a 15% PBG. The corresponding electromagnetic density of states is shown in **Figure 4**. This structure is amenable to micro-fabrication using a technique called Glancing Angle Deposition (GLAD) [16,17].
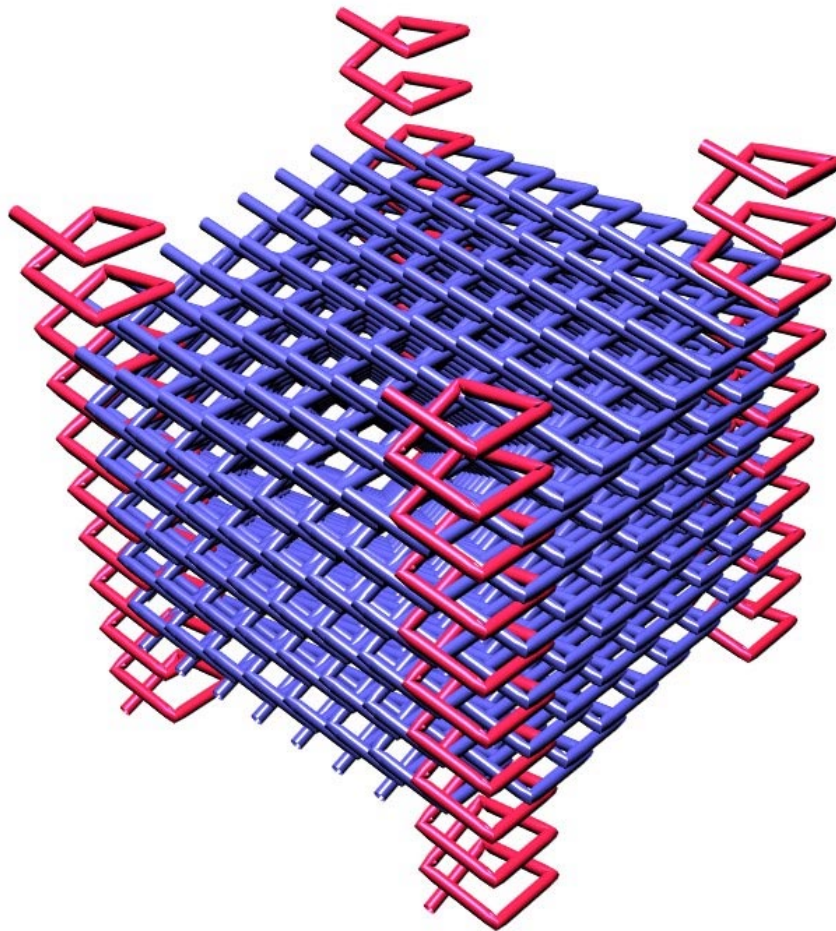

Figure 3. The Tetragonal lattice of Square Spiral posts exhibits a complete 3D PBG and can be synthesized using a glancing angle deposition (GLAD) method. This chiral structure consists of slightly overlapping square spiral posts grown on a 2D substrate that is initially seeded with a square lattice of growth centers. Computer controlled motion of the substrate leads to spiraling growth of the posts. A large and robust 3D PBG emerges between the 4th and 5th bands of the photon dispersion. The "inverse structure" consisting of air posts in a solid background exhibits an even larger 3D PBG.
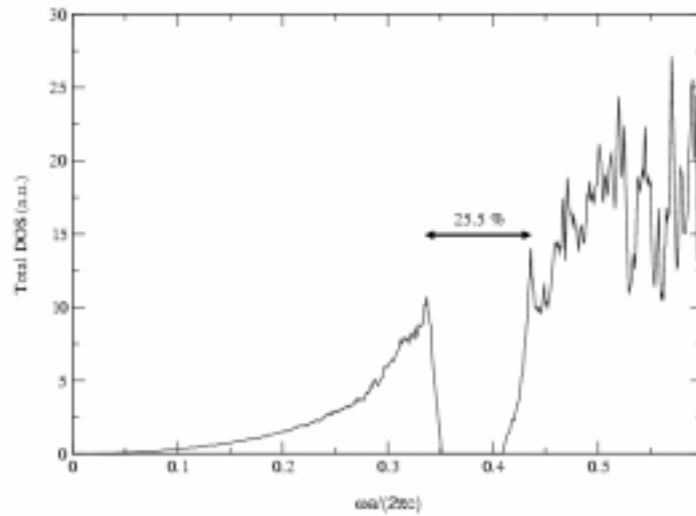
Figure 4. Electromagnetic density of states as a function of frequency for the tetragonal square spiral structure of **Figure 3**. The total 3D density of states (DOS) vanishes over an interval of 15% of the center frequency between the 4th and 5th photon dispersion bands. In this interval, the material is "emptier than vacuum" in the sense that even the zero point (quantum) fluctuations of the electromagnetic field have been eliminated. The size of the (larger) pseudogap over which the DOS differs significantly from that of ordinary vacuum is roughly 25% of the center frequency.

Simple applications of PBG materials can be found in the microwave to millimeter wave range. For instance, an antenna mounted on a conventional dielectric substrate emits the majority of its radiation into the substrate itself. If the substrate is engineered into the form of a PBG material with a gap at the radiation frequency, the losses can be minimized, leading to highly directional transmitters [18,19]. Other applications include optical filters with tailor made characteristics [20] and cladding material for preventing losses in waveguide structures that contain bends or junctions [21,22,23]. Nevertheless, it is for visible and near-infrared frequencies where PBG materials are likely to have their most important impact. For example, applications in telecommunications require the fabrication of PBG materials with a gap centered in the 1.3-1.5μm range, where there is minimal absorption of light in silica based optical fibers. These applications include the design of ultra-compact lasers that emit coherent light with almost no pumping threshold, all-optical switching fabrics for routing data along the internet, optical switches with an on-off cycle time of less than a trillionth of a second, and all-optical transistors.

PBG materials also represent a new frontier in fundamental aspects of quantum and nonlinear optics. While linear wave propagation is absent in the gap of a PBG material, nonlinear propagation effects can still occur [24,25,26]. When the backbone of the PBG exhibits a nonlinear refractive index (that depends on the intensity of the electromagnetic wave field) certain high intensity "light bullets" (solitary waves) can pass through the material even at frequencies within the gap. In addition, PBG materials exhibit novel quantum optical features, related to the drastic alteration of the photon density of states (DOS). A vanishing DOS leads to bound photon-atom states, [27,28] suppressed

7

spontaneous emission [4,5,29,30] and strong localization of photons [3,27,28,31]. Localization of photons implies that emission of light from an initially excited atom occurs in a way that is very different from that in ordinary vacuum. In a PBG material, the atom has a long time memory of the fact that it was optically excited at an earlier time. One consequence of such memory and intrinsic feedback is that lasing can occur at a photonic band edge without recourse to a standard laser cavity involving a pair of mirrors. Other novel phenomena predicted to occur in a PBG material include: (i) collective switching of two-level atoms from ground to excited state with low intensity applied laser fields leading to all-optical transistor action [32], (ii) single atom memory effects for possible quantum computer applications [33], and (iii) low threshold and other anomalous nonlinear optical response [34].

3. Two-Dimensional PBG materials

In many applications, the polarization state of guided light can be fixed in a particular direction and only the passive optical guiding characteristics of a PBG material come into play. Two-dimensional (2D) periodic microstructures are often sufficient for such applications. For 2D periodic dielectrics, advanced planar microstructuring techniques borrowed from semiconductor technology can greatly simplify the fabrication process. Such structures are referred to as photonic crystals exhibiting a 2D PBG or 2D PBG materials. The "aspect ratio" of a 2D PBG material is defined as the ratio of the sample depth (vertical direction) to the lattice constant (transverse direction).

High-quality photonic crystals with aspect ratios of up to 5:1 can be manufactured through plasma etching or electron beam lithography techniques [35,36,37]. These are sometimes referred to as membrane structures. Alternatively, high aspect ratio 2D PBG structures can be manufactured by photo- electrochemically growing ordered macropores into a silicon wafer [38,39]. With these 2D PBG materials aspect ratios of 200:1 and 2D band gaps centered at wavelengths in the 1.3-1.5µm have been achieved [40].
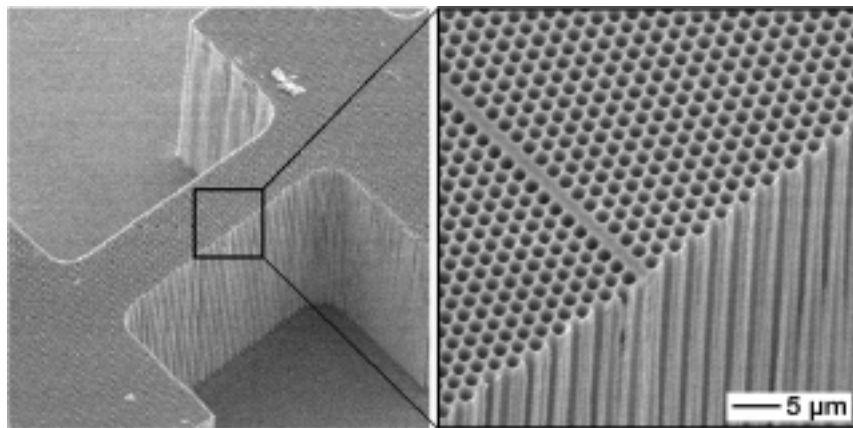

Figure 5. Laterally structured sample of macro-porous silicon material with an incorporated defect line. The H-like structure facilitates the positioning of a fiber for the coupling in and out of light. The lattice constant is 1.5 µm and the pore height is 100µm. For a suitably focused beam, the structure represents a truly 2-D PBG material with a band gap around 3µm. (courtesy of Ulrich Gösele, Max-Planck Institute for Microstructure Physics, Halle, Germany).

The quality of 2D PBG materials synthesized using the photo-electrochemical process is shown in **Figure 5**. Here, we depict a bar of macroporous silicon consisting of 22 pore

layers with a lattice constant of 1.5 μm. This structure exhibits a 2D PBG centered near 3 μm. That is to say there is a band of frequencies over which light polarized with either the electric field (E-polarization) or magnetic field (H-polarization) parallel to the pores cannot propagate through the material. During the fabrication process of a 2D PBG material, light paths within the gap can be engineered through the introduction of defects. For instance, if a single pore is modified or left out altogether (by placing an etch mask over silicon wafer), an optical microcavity is formed and leads to a localized mode of light inside the PBG. A chain of such point defects can act as a linear waveguide channel [23,41] and facilitate very sharp wave guide bends. It can also provide ultra-small beam-splitters, Mach-Zehnder interferometers, and functional micro-optical elements such as wavelength add-drop filters [42]. Some defect structures [43] are shown in **Figure 6**.
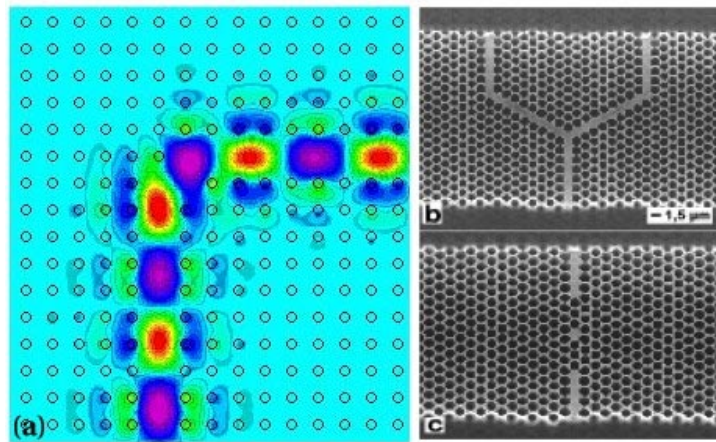

Figure 6. **(a)** Sharp bend waveguide channel in a 2D photonic crystal. The colors show the propagation of a electromagnetic mode around the bend with no reflection or scattering losses (courtesy of J.D.Joannopoulos, Massachusetts Institute of Technology). **(b,c)** Electron micrographs of other defect structures realized in macroporous silicon with a lattice constant of 1.5 μm. The split waveguide in **(b)** may be used as an optical interferometer and the air holes within the waveguide channel **(c)** can be used as Bragg mirrors to isolate a resonator cavity within the waveguide. (courtesy of Max-Planck Institute for Microstructure Physics, Halle, Germany).

4. Two-Dimensional Photonic Crystal Devices

An add-drop filter for a wavelength division multiplexed (WDM) communication system is depicted in **Figure 7**. Here, light from an optical fiber carrying many different frequencies, F1, F2,… is inserted into a 2D PBG structure by means of a wave guide channel (missing row of holes). The frequencies F1, F2,… lie within the 2D PBG and cannot escape from the waveguide channel except in places where the periodicity of the background pores is disrupted by means of defects. For example, a hole that is larger than all the other background holes can act as a resonator which picks of a particular frequency, say F1, from the wave guide channel, while allowing other frequencies to propagate freely along the wave guide. Channel drop tunneling though localized defect modes with more sophisticated geometries have already been designed [42] and tested [44]. A collection of such defects could serve to pick up a band of frequencies and route them to a specified destination.
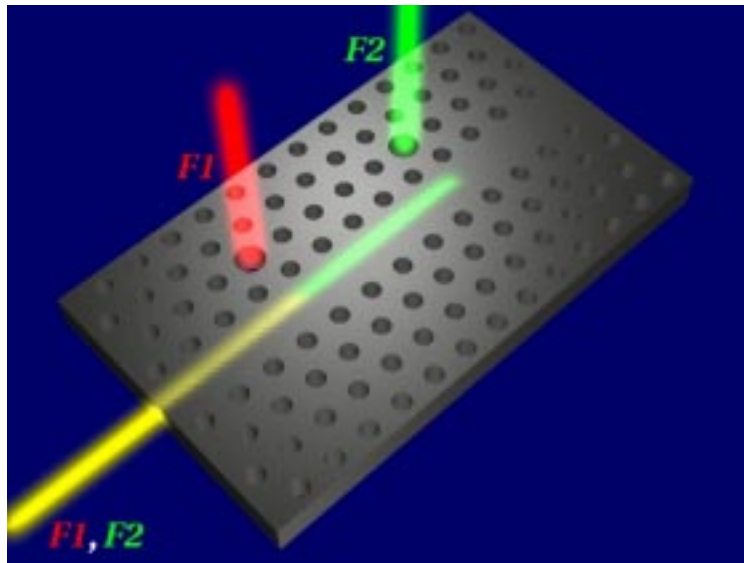
Figure 7. Add-drop filter for a dense wavelength division multiplexed optical communication system. Multiple streams of data carried at different frequencies F1, F2, etc. (**yellow**) enter the optical micro-chip from an external optical fiber and are carried through a wave guide channel (missing row of pores). Data streams at frequency F1 (**red**) and F2 (**green**) tunnel into localized defect modes and are routed to different destinations. The frequency of the drop filter is defined by the defect pore diameter which is different from the pore diameter of the background photonic crystal.

A number of prototype "active" devices based on 2D PBG hetero-structures have been designed and tested. For example 2D photonic crystal micro-lasers already rival the best available micro-cavity lasers both in size and performance. For a 2D PBG the localization of light and control of spontaneous emission from excited two-level systems is incomplete. Nevertheless, low threshold lasing from ultra-compact devices has been demonstrated [35,45].

Figure 8 depicts two distinct types of micro-lasers. The first (shown in **Figure 8a**) is a "band edge micro-laser" in which light emission from electrically injected electron-hole pairs in a multiple quantum well array occurs near the band edge of a 2D PBG. It has been predicted [29] that strong feedback and memory effects accompany collective light emission near the photonic band edge. Near a true 3D photonic band edge, this would lead to lasing without a conventional optical cavity [31]. A precursor to this effect is seen in the 2D band edge micro-laser in which lasing occurs preferentially at the 2D photonic band edge [45] even though the emission from the active region has a broad frequency distribution.

The second type of micro-laser (shown in **Figure 8b**) utilizes a localized state defect mode as a laser cavity [35]. Here, the localized electromagnetic mode is associated with a missing hole in the 2D triangular lattice. This particular structure has been proposed as the "world's smallest micro-laser" with a cavity volume of 0.03 cubic microns. Spontaneous emission from electron-hole pair recombination in the multiple quantum well active region occurs preferentially into the localized state. Since the photonic crystal is two-dimensional, spontaneous emission is not exclusive to the lasing mode. This results in a finite pumping threshold before lasing occurs.
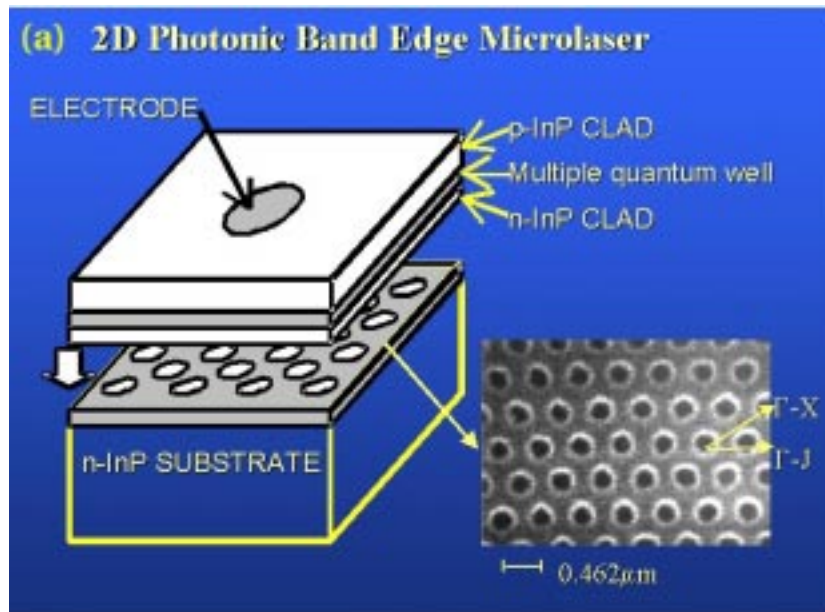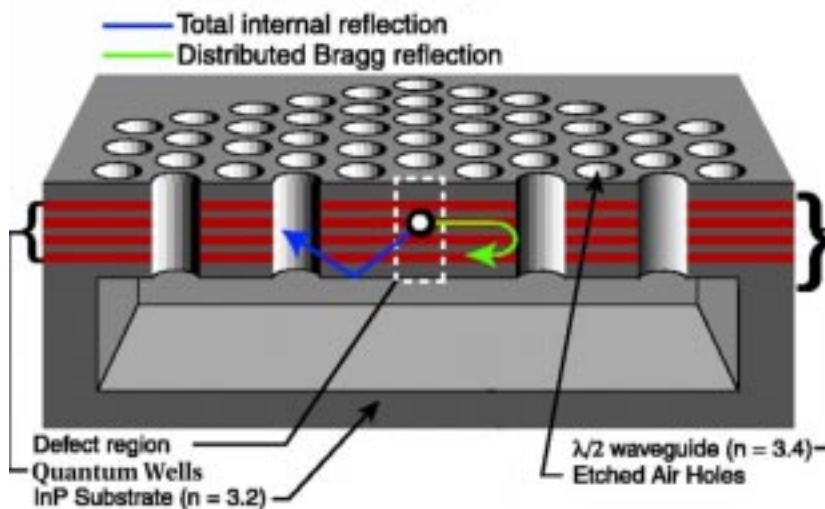
Figure 8. Architectures for 2D photonic crystal micro-lasers. **(a)** The Band Edge micro-laser utilizes the unique feedback and memory effects associated with a photonic band edge and stimulated emission (arising from electron-hole recombination) from the multiple quantum well active region occurs preferentially at the band edge. There is no defect mode engineered in the 2D PBG. (courtesy of S. Noda, Kyoto University). **(b)** Defect Mode micro-laser requires the engineering of a localized state of light within the 2D PBG. This is created through a missing pore in the 2D photonic crystal. Stimulated emission from the multiple quantum well active region occurs preferentially into the localized mode. (courtesy of Axel Scherer, California Institute of Technology).

5. Synthesis of Three-dimensional PBG materials

While 2D PBG materials can confine light in two spatial dimensions, 3D PBG materials facilitate complete localization of light and can facilitate complete inhibition of spontaneous emission of light from atoms, molecules, and other excitations. If the transition frequency from such an atom lies within a 3D PBG, the photon that would normally be emitted and escape from the atom forms a bound state to the atom. Such feedback effects have important consequences on laser action from a collection of atoms. Indeed lasing may occur near a photonic band edge even without the need for mirrors as in a conventional laser cavity.

5.1 Layer-by-layer structures

The "woodpile" structure [9,10] represents a three-dimensional PBG material that lends itself to layer-by-layer fabrication. It resembles (see **Figure 9**) a criss-crossed stack of wooden logs, where in each layer the logs are in parallel orientation to each other. To fabricate one layer of the stack, a SiO_2-layer is grown on a substrate wafer, then patterned and etched. Next, the resulting trenches are filled with a high-index material such as silicon or GaAs and the surface of the wafer is polished in order to allow the next SiO_2 layer to be grown. The logs of second nearest layers are displaced midway between the logs of the original layer. As a consequence, 4 layers are necessary to obtain one unit cell in the stacking direction. In a final step, the SiO_2 is removed through a selective etching process leaving behind the high-index logs.

Recent works report about the successful fabrication of such a layer-by-layer PBG material made from silicon with a PBG around 1.5 μm [46]. However, this structure consisted of only 5 layers in the stacking direction. Instead of depositing successively more layers, wafer-bonding technology may be applied to single-layer substrates [47]. Bonding together two single-layer substrates and subsequent removal of the upper substrate results in a double-layer structure. The ensuing technique is multiplicative but tedious and expensive. To date, this type of complex microlithography has lead to the successful fabrication of an 8 layer structure (2 unit cells) in the stacking direction.

Integrated Optical Circuitry On a 3D PBG Microchip

Optical Modulator

Zero-Threshold Laser Array

Ultra-small Multi-Wavelength Light Source
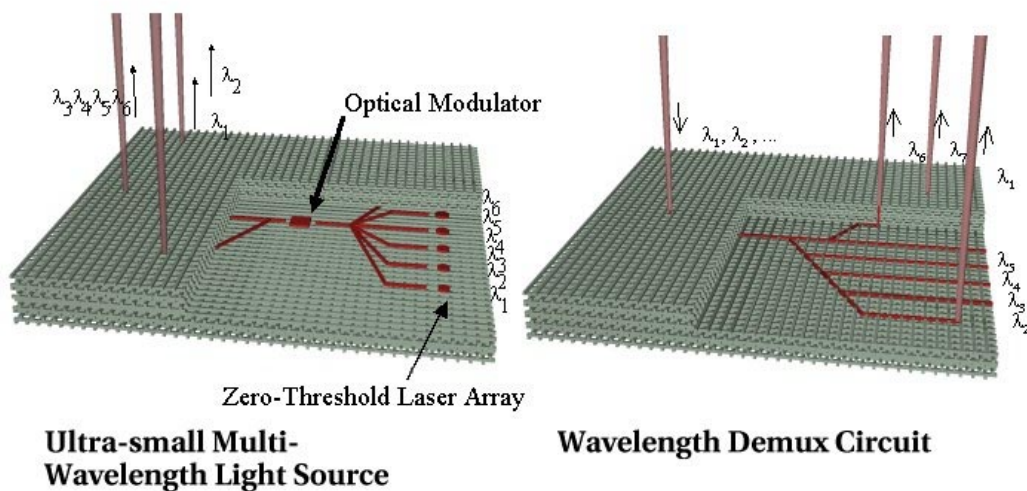
Wavelength Demux Circuit

Figure 9. An artist's conception of a 3D PBG woodpile structure into which a micro-laser array and de-multiplexing (DEMUX) circuit have been integrated. (courtesy of S. Noda, Kyoto University, Japan).

5.2 Self-organizing structures

In three dimensions a number of large-scale self-assembling periodic structures already exist. These include colloidal systems [48,49] and artificial opals [50,51]. Unfortunately, these readily available materials do not satisfy the necessary criteria of high index contrast and correct network topology to produce a complete PBG. Theoretical studies, however, indicate the possibility of a complete PBG in closely related structures. Face centered cubic lattices consisting of low dielectric inclusions in a connected high dielectric network (henceforth called inverse structures) [52] can exhibit small PBGs. The recipe of producing inverse structures from artificial opals is to infiltrate them with a high dielectric material such as silicon [53] and to subsequently etch out the SiO_2 spheres, leaving behind a connected network of high dielectric material with filling ratios of about 26% by volume. Such a "Swiss cheese structures" with air voids in a silicon backbone is displayed in **Figure 10**. This large-scale inverse opal PBG material exhibits a complete 5% PBG relative to its center frequency at 1.5 μm [53]. The etching out of the SiO_2 provides the necessary dielectric contrast for the emergence of a complete 3D PBG. Moreover, the presence of air voids rather than solid SiO_2 may allow the injection of atomic vapors with which quantum optical experiments can be carried out. It also facilitates the infiltration of optically anisotropic materials such as nematic liquid crystals for the realization of electro-optic tuning effects and enables the infiltration of active materials such as conjugated polymers and dyes for laser applications.
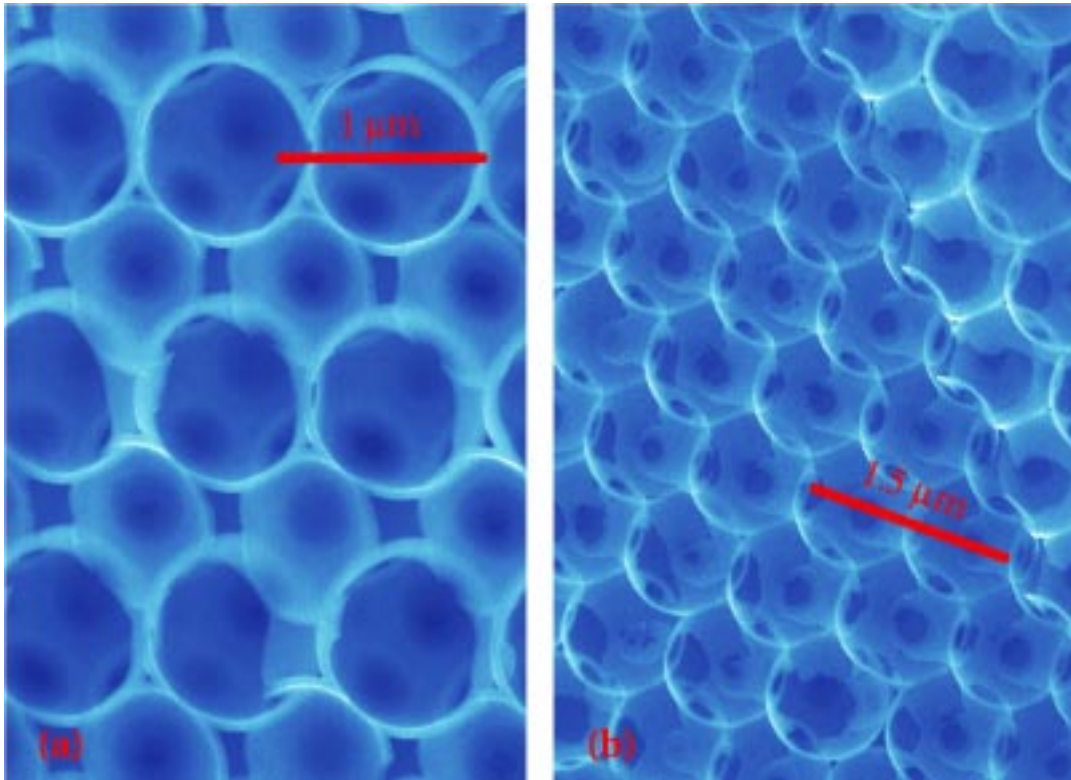
Figure 10. Scanning Electron Microscope (SEM) pictures of cross section along **(a)** the cubic (110)-direction and **(b)** the cubic (111)-direction of a silicon inverse opal with a complete 5% PBG around 1.5 µm. The structure has been obtained through an infiltration of an artificial opal with silicon (light shaded regions) and subsequent removal of the SiO_2 spheres of the opal. The air sphere diameter is 870 nanometers. Clearly visible is the incomplete infiltration (diamond shaped voids between spheres) and the effect of sintering the artificial opal prior to infiltration (small holes connecting adjacent spheres).

6. Quantum and Nonlinear Optics in 3D PBG Materials

Photonic band gap materials represent a fundamentally new paradigm for low threshold nonlinear optical phenomena. The PBG affects the light-matter interaction in a fundamental way. For instance, if the transition frequency of an excited atom embedded in such a material lies within the complete PBG, spontaneous emission may be completely suppressed and a bound photon-atom state is formed instead [27,28]. Based on these principles numerous applications for active devices have been suggested. Two illustrative examples are given below.

6.1 Low Threshold Resonant Nonlinear Optics

The ability to achieve ultrafast nonlinear optical response in a non-absorbing material is crucial in applications such as all-optical switches and other nonlinear devices for integrated optical circuits. In a conventional Fabry-Perot device containing a weakly nonlinear layer, transistor-like response requires relatively high intensity laser fields. The situation may be dramatically different in the context of a three-dimensional PBG material where the inhibition of spontaneous emission from atoms and molecules is essentially complete.

Consider the injection of a classical monochromatic electromagnetic wave of frequency ω into a 3D PBG material by means of a single mode wave guide channel.

Suppose this wave guide channel contains a small active region of optically excitable two-level systems (confined electron-hole pair excitations or atoms) with a radiative transition at frequency ω_0 such that the detuning $\Delta = \omega - \omega_0 \square \ \omega_0$. For weak fields, the response of the two-level atom is that of a simple harmonic oscillator since the atom spends the majority of time in its ground state. Whenever the external field excites the atom, it quickly returns to its ground state due to the rapid rate of spontaneous emission. As the external field intensity is increased, the upper state population increases and eventually saturates. This is associated with nonlinear response. The appropriate mechanical analogy for the quantum two-level system is no longer a classical harmonic oscillator, but rather a simple pendulum (atomic Bloch vector) whose coordinates are given by the different components of the 2×2 atomic density matrix. Small angle oscillation of the atomic Bloch vector describes linear response whereas large angle oscillations probe the nonlinear susceptibility of the atom. The threshold external field required to probe nonlinear response is called the line center saturation field strength E_s^0 which is related to the rate of spontaneous emission $1/T_1$ by the formula [54]:

$$| E_s^{\ 0} |^2 = \frac{\hbar^2}{4\mu_{ba} T_1 T_2} \tag{3}$$

Here, $1/T_2$ is the rate of dipolar dephasing and μ_{ba} is the electric dipole transition matrix element for the atom. In ordinary vacuum (as opposed to our 3D PBG material), the textbook formula [54] for the nonlinear susceptibility is:

$$\chi = \chi_0 \frac{\Delta T_2 - i}{1 + \Delta^2 T_2^{\ 2} + | E |^2 \ / | E_s^{\ 0} |^2} \tag{4}$$

Here, χ_0 is a frequency independent constant, $\Delta = \omega - \omega_0$ is the detuning of the external field of amplitude E and frequency ω. Clearly, the susceptibility, χ, is independent of E for $E \ \square \ E_s^{\ 0}$ whereas it has a highly nonlinear dependence on E for $E > E_s^{\ 0}$. This widely accepted picture of nonlinear optical response in ordinary materials is no longer applicable in a three-dimensional PBG material in which two-level atoms have a radiative transition at frequency ω_0 that lies within the PBG. Inside a PBG, the rate $1/T_1$ and accordingly the threshold intensity $|E_s^0|^2$ formally vanish. While this is suggestive of low threshold nonlinear optical response, it is in fact an indication that the entire derivation of the conventional susceptibility, Eq. 4, must be carefully re-examined in the context of the PBG. In particular, Eq. 4 is based on retaining only the leading order photon-atom interaction, namely spontaneous emission. In the PBG, this leading process is almost absent. Therefore, it is necessary to consider the next process, namely resonance dipole-dipole interaction (RDDI) between a pair of two-level atoms. A straightforward derivation [34] of the nonlinear susceptibility in this context leads to some remarkable effects. For example, it is possible (at relatively low field intensities) to completely saturate the imaginary (absorptive) part of χ while retaining a large real part for χ. This arises in a situation where a collection of atoms inside a PBG interact randomly by RDDI and an external field enters the material through a small number of defect (wave guide) modes. Due to the inhibition of spontaneous emission, the single atom absorptive transition is saturated at nearly the one-photon level. However, due to the random nature

of RDDI, the induced atomic dipoles are randomly oriented and remain highly susceptible to alignment (macroscopic polarization) by the external field.

6.2 Collective Switching and Transistor Effects

A second illustration of novel radiation-matter interaction in a PBG material arises if a collection of two-level atoms is selected such that their radiative transition lies very close to a photonic band edge. Near the photonic band edge, the electromagnetic density of states varies rapidly with frequency and the spontaneous emission processes cannot be adequately described using Fermi's Golden Rule. We refer to the case in which the density of states exhibits singularities or abrupt variation as a "colored vacuum". In the colored vacuum of a photonic band edge it is possible to achieve population inversion for a collection of two-level atoms driven by a weak coherent pump laser field. As the number of atoms in a cubic wavelength increases, this switching from a passive medium (most atoms in ground state) to an active medium (population inverted) occurs sharply as the external pump laser intensity is increased. In the region of this collective jump in atomic population, there is a large differential optical gain. If the pump laser intensity is chosen slightly below threshold for population inversion, a second control laser field can be introduced to act as a gate which determines whether the pump laser field is either attenuated or amplified by the medium (see **Figure 11**). Since all of these processes involve coherent radiation-atom interactions, this system may form the basis of a low threshold optical switch or all-optical transistor [32].

When a coherent laser field with average incident energy density W and frequency ω interacts with a collection of N two-level atoms in ordinary vacuum, the steady state behavior of the system is governed by the well-known Einstein rate equations. These equations implicitly make use of the smooth nature of the vacuum density of states $N(\omega) = \omega^2/(\pi^2 c^3)$ in the vicinity of the atomic transition frequency $\omega \approx \omega_0$. In steady state equilibrium, the ratio of the number of excited atoms, N_2, to the total number of atoms is given by [55]:

$$\frac{N_2}{N} = \frac{W}{\hbar \omega N(\omega) + 2W} \tag{5}$$

Clearly, as W increases, the maximum value of N_2/N is less than $1/2$. In other words, it is not possible to invert a collection of two-level atoms with a coherent laser field. From a more quantum mechanical point of view, the external laser field may be regarded as consisting of a large collection of n photons. The atom-radiation field interaction Hamiltonian, H_{int}, breaks the degeneracy between a state consisting of a given atom in its excited state and (n-1) photons in the radiation field (which we denote by the ket $|2,n-1>$) and a state consisting of the given atom in its ground state and n-photons in the radiation field (which we denote by the ket $|1,n>$). The matrix element $<2,n-1|H_{int}|1,n>$ is nonzero and the true eigenstates of the system are called dressed atomic states. These "dressed states" are linear combinations of the "bare" kets listed above. Accordingly, the eigenenergies of the dressed states are shifted from their bare values by an amount $\Delta \sim \mu_{ba}|E|/h$ (Rabi frequency) where μ_{ba} is the atomic dipole matrix element and $|E|$ is the laser field amplitude. This leads to the well-known Mollow fluorescence spectrum in

ordinary vacuum [55]. Rather than a single peak in the atomic spectrum centered at the bare atomic transition frequency ω_0, the fluorescence spectrum exhibits three peaks centered at ω_0, $\omega_0+\Delta$, and $\omega_0-\Delta$.

The Einstein rate equation picture of the steady state atomic inversion, Eq. 5, relies on the fact that the vacuum density of electromagnetic modes $N(\omega)$ is relatively smooth on the scale of Δ. That is to say, the Einstein picture assumes that the rate of spontaneous emission in the Mollow sidebands at $\omega_0+\Delta$ and $\omega_0-\Delta$ is roughly the same. In ordinary vacuum ($N(\omega) = \omega^2/(\pi^2 c^3)$) this assumption is easily satisfied. Moreover, in ordinary vacuum, very high intensity fields are required to observe any Mollow splitting whatsoever. The situation is dramatically different in a PBG material where the density of states itself exhibits rapid variation from frequency $\omega_0-\Delta$ to $\omega_0+\Delta$. Another striking property of the photonic band edge is that atomic line splitting may be achieved with very low intensity fields. In particular, vacuum Rabi splitting of an atomic transition placed directly at the band edge has been predicted [27,28,29]. In other words, at a band edge, significant splitting can be expected in an atomic line even in the presence of a single photon! This leads to a dramatic modification of the Einstein picture.

In a weak applied laser field, atoms with a bare transition frequency ω_0 which coincides with a photonic band edge will exhibit a pair of dressed states that straddle the band edge [27,28,29]. These two spectral sidebands will experience vastly different rates of spontaneous emission. The spectral component that is pulled into the gap will exhibit negligible decay. This component corresponds to a photon-atom bound state [27]. The spectral component that is pushed away from the gap can exhibit emission into the allowed modes of the photonic band. Population inversion for a collection of such atoms can readily be achieved by an external laser field due to trapping of excitation energy in the photon-atom bound state component [32].
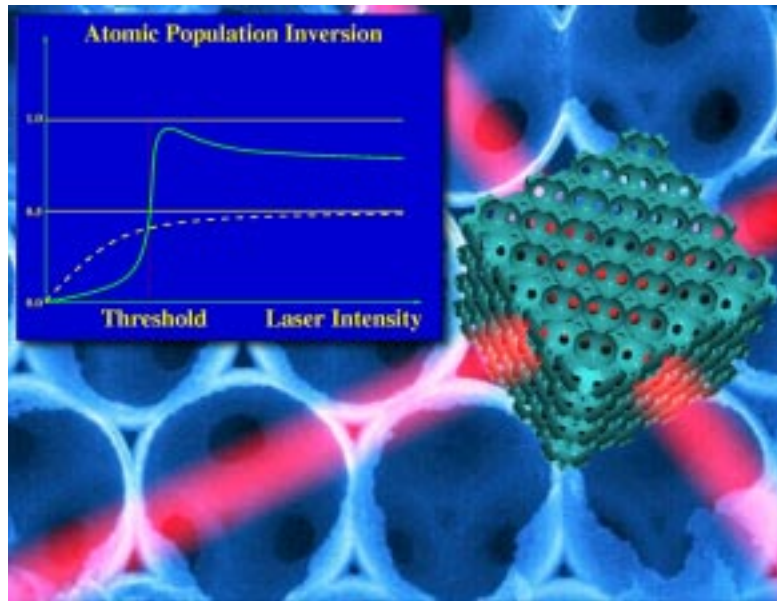
Figure 11. Micro-photonic all-optical transistor may consist of an active region buried in the intersection of two wave-guide channels in a 3D PBG material. The two-level systems ("atoms") in the active region are coherently pumped and controlled by laser beams passing through the wave guides. In addition, the 3D PBG material is chosen to exhibit an abrupt variation in the photon density of states near the transition frequency of the atoms. This leads to atomic "population inversion" through coherent pumping, an effect which is forbidden in ordinary vacuum. The inversion threshold is characterized by a narrow region of large differential optical gain (solid curve in the inset). A second, "control laser" allows the device to pass through this threshold region leading to strong amplification of the output signal. In ordinary vacuum, population inversion is unattainable (dashed curve in the inset).

The resulting collective switch in atomic population as a function of applied field intensity is depicted schematically within the inset of **Figure 11**. Details of this result may be found in reference [32]. This transition becomes increasingly sharp as the number of atoms increases and defines a region of large differential optical gain. It is expected that the collective switch can be achieved for a very low applied field and that the switching effect is robust with respect to variety of dephasing effects due to lattice vibrations in the host PBG material.

7. Tunable PBG materials

For many applications it is advantageous to obtain some degree of tunability of the photonic band structure through electro-optic effects. This may be useful in routing of signals through an optical communication network and provide flexibility to reconfigure the routing as conditions in the network change. One of the great advantages of PBG materials is that by volume, most of the material consists of pores. These pores can be infiltrated with other electro-optically active materials which enable reconfiguration of the underlying photonic band structure either globally or locally. Tunability may be obtained by controlling one or several forms of optical anisotropy of the constituent materials. For example the science of liquid crystals has spawned an entire industry related to these electro-optic effects. Inverse opal structures provide a highly efficient scattering system as illustrated by the complete PBG of silicon inverse opals (**Figure 10** and **Figure 11**). The nearly 75% empty volume of this structure is ideally suited for infiltration by a low refractive index liquid crystal with strong optical anisotropy making

them efficacious for electro-optic tuning effects. In particular, a change in the orientation of the nematic director field with respect to the inverse opal backbone by an external electric field can completely open or close the full, three-dimensional PBG [56]. This clearly demonstrates an electro-optic shutter effect to the PBG which may be realized by external means. The resulting tunability of spontaneous emission, waveguiding effects, and light localization may considerably enhance the technological value of a composite liquid crystal PBG material over and above that of either a bulk liquid crystal or a conventional PBG material by itself. A tunable optical microchip which routes light from a set of optical fibers is shown in **Figure 12**.
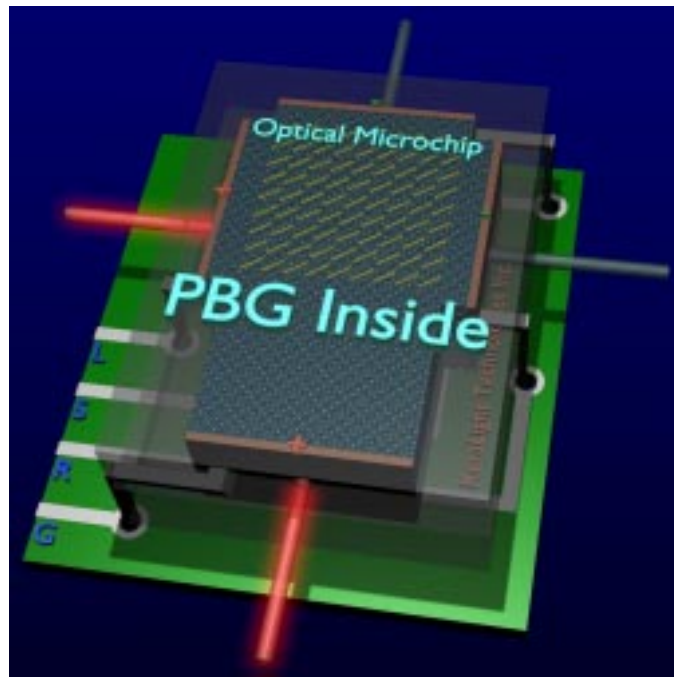

Figure 12. Artist's depiction of an electro-actively tunable PBG routing device. Here the PBG material has been infiltrated with an optically anisotropic material (such as a liquid crystal) exhibiting a large electro-optic response. When a voltage is applied to the electro-optically tunable PBG, the polarization state (yellow arrows) can be rotated, leading to corresponding shifts in the photonic band structure. This allows light from an optical fiber to be routed into one of several output fibers.

8. Outlook

The synergetic interplay between advanced material science, theoretical analysis and modern spectroscopy has been and continues to be the driving force for the field of PBG materials. Recent advances in micro-structuring technology have allowed the realization and controlled engineering of three-dimensional PBG structures at the near IR as well as the visible frequency spectrum of electromagnetic radiation. In a parallel development, the theoretical description of PBG materials has matured to the point where it provides a reliable interpretative as well as predictive tool to both material synthesis and spectroscopic analysis of these novel semiconductors for light. The current state of PBG research suggests that this field is at a stage comparable to the early years of semiconductor technology shortly before the invention of the solid state electronic transistor by W. Shockley, J. Bardeen, and W.H. Brattain. If this analogy continues to

hold, one may find the PBG materials at the heart of a 21st century revolution in optical information technology similar to the revolution in electronics we have witnessed over the latter half of the 20th century.

References

[1] S. John, Phys. Rev. Lett. **53**, 2169 (1984)

[2] P.W. Anderson, Phil. Mag. **B52**, 505 (1985)

[3] S. John, Phys. Rev. Lett. **58**, 2486 (1987)

[4] E. Yablonovitch, Phys. Rev. Lett. **58**, 2059 (1987)

[5] V.P. Bykov, Sov. J. Quant. Electron. **4**, 861 (1975)

[6] S. John and R. Rangarajan, Phys. Rev. B **38**, 10101 (1988)

[7] K.-M. Ho, C.T. Chan, and C.M. Soukoulis, Phys. Rev. Lett. **65**, 3152 (1990)

[8] E. Yablonovitch, T.J. Gmitter, and K.M. Leung, Phys. Rev. Lett. **67**, 2295 (1991)

[9] K.-M. Ho, C.T. Chan, C.M. Soukoulis, R. Biswas, and M. Sigalas, Sol. Stat. Commun. **89**, 413 (1993)

[10] C.T. Chan, S. Datta, K.-M. Ho, C.M. Soukoulis, Phys. Rev. B **50**, R1988 (1994)

[11] S. Fan, P.R. Villeneuve, R.D. Meade, and J.D. Joannopoulos, Appl. Phys. Lett. **65**, 1466 (1994)

[12] K.M. Leung, Phys. Rev. B (Brief Reports) **56**, 3517 (1997)

[13] E. Özbay, A. Abeyta, G. Tuttle, M. Tringides, R. Biswas, C.T. Chan, C.M. Soukoulis, and K.M. Ho, Phys. Rev. B **50**, 1945 (1994)

[14] E. Özbay, E. Michel, G. Tuttle, R.Biswas, M. Sigalas, and K.M. Ho Appl. Phys. Lett. **64**, 2059 (1994)

[15] E. Özbay, G. Tuttle, J.S. McCalmont, R. Biswas, C.M. Soukoulis, and K.M. Ho, Appl. Phys. Lett. **67**, 1969 (1995)

[16] K. Robbie, M. J. Brett, Nature, **384**, 616 (1996)

[17] K. Robbie, J. C. Sit, M. Brett, J. Vac. Sci. Technol. B **16**, 1115 (1998)

[18] E.R. Brown, C.D. Parker, and O.B. McMahon, Appl. Phys. Lett. **64**, 3345 (1994)

[19] S.D. Cheung et al., Appl. Phys. Lett. **67**, 3399 (1995)

[20] M. Sigalas, J.S. McCalmont, K.M. Ho, and G. Tuttle, Appl. Phys. Lett. **68**, 3525 (1996)

[21] A. Mekis, J.C. Chen, I. Kurland, S. Fan, P. Villeneuve, and J.D. Joannopoulos, Phys. Rev. Lett. **77**, 3787 (1996)

[22] S.-Y. Lin, V.M. Hietala, S.K. Lyo, and A. Zaslavsky, Appl. Phys. Lett. **68**, 3233 (1996)

[23] K. Sakoda, T. Ueta, and K. Ohtaka, Phys. Rev. B **56**, 14905 (1997)

[24] S. John, and N. Aközbek, Phys. Rev. Lett. **71**, 1168 (1993)

[25] N. Aközbek, and S. John, Phys. Rev. E **57**, 2287 (1998)

[26] N. Aközbek, and S. John, Phys. Rev. E **58**, 3876 (1998)

[27] S. John, and J. Wang, Phys. Rev. Lett. **64**, 2418 (1990)

[28] S. John, and J. Wang, Phys. Rev. B **43**, 12772 (1991)

[29] S. John, and T. Quang, Phys. Rev. A **50**, 1764 (1994)

[30] S. Bay, P. Lambropoulos, and K. Molmer, Opt. Comm. **132**, 257 (1996)

[31] S. John, and T. Quang, Phys. Rev. Lett. **74**, 3419 (1995)

[32] S. John, and T. Quang, Phys. Rev. Lett. **78**, 1888 (1997)

[33] T. Quang, M. Woldeyohannes, S. John, and G.S. Agarval, Phys. Rev. Lett **79**, 5238 (1997)

[34] S. John, and T. Quang, Phys. Rev. Lett. **76**, 2484 (1996)

[35] O. Painter et al., Science **284**, 1819 (1999)

[36] P.L. Philips et al., J. Appl. Phys. **85**, 6337 (1999)

[37] D. Labilloy et al., Phys. Rev. B **59**, 1649 (1999)

[38] U. Grüning, V. Lehmann, and C.M. Engelhardt, Appl. Phys. Lett. **66**, 3254 (1995)

[39] U. Grüning, V. Lehman, S. Ottow, and K. Busch, Appl. Phys. Lett. **68**, 747 (1996)

[40] J.Schilling, A. Birner, F. Müller, R.B. Wehrspohn, R. Hillebrand, U. Gösele, K. Busch, S. John, S.W. Leonard, and H.M. van Driel, to be published in Optical Materials (2001)

[41] S.W. Leonard, H.M. van Driel, A. Birner, U. Gösele, and P.R. Villeneuve, Opt. Lett. **25**, 1550 (2000)

[42] S. Fan, P. R. Villeneuve, J. D. Joannopoulos, H. A. Haus, Phys. Rev. Lett. **80**, 960 (1998)

[43] A. Birner, U. Grüning, S. Ottow, A. Schneider, F. Müller, V. Lehmann, H. Föll, and U. Gösele, Phys. Stat. Sol. (a) **165**, 111 (1998)

[44] S. Noda, A. Chutinan, M. Imada, Nature, **407**, 608 (2000)

[45] M. Imada, S. Noda, A. Chutinan, T. Tokuda, M. Murata, G. Sasaki, Appl. Phys. Lett. **75**, 316 (1999)

[46] S.-Y. Lin and J. G. Fleming, J. Lightwave Technology **17**, 1944 (1999)

[47] S. Noda, N. Yamamoto, M. Imada, H. Kobayashi, and M. Okano, J. Lightwave Technology **17**, 1948 (1999)

[48] I.I. Tarhan, and G.H. Watson, Phys. Rev. Lett. **76**, 315 (1996)

[49] W.L. Vos, R. Sprik, A. van Blaaaderen, A. Imhof, A. Lagendijk, and G.H. Weydam, Phys. Rev. B **53**, 16231 (1996)

[50] Yu.A. Vlasov et al., Phys. Rev. B **55**, R13357 (1997)

[51] H. Miguez et al., Appl. Phys. Lett. **71**, 1148 (1997)

[52] H.S. Sözüer, J.W. Haus, and R. Inguva, Phys. Rev. B **45**, 13962 (1992)

[53] A. Blanco et al., Nature (London) **405**, 437 (2000)

[54] R. Boyd, *Nonlinear Optics*, Academic Press 1992

[55] R. Loudon, *The Quantum Theory of Light*, Clarendon 1983

[56] K. Busch and S. John, Phys. Rev. Lett. **83**, 967 (1999)